Project 065(A) Fuel Testing Approaches for Rapid Jet Fuel Prescreening

Washington State University

Project Lead Investigator

Joshua Heyne
Bioproducts, Sciences, and Engineering Laboratory Director, Associate Professor
School of Engineering and Applied Science
Washington State University
2710 Crimson Way, Richland, WA 99354
509-372-7461
joshua.heyne@wsu.edu

University Participants

Washington State University (WSU)

- P.I.: Joshua Heyne
- FAA Award Number: 13-C-AJFE-UD, Amendments 26, 31, 34, and 42
- Period of Performance: October 1, 2024, through September 30, 2025. Cost share is from the German Aerospace Center (DLR).
- Task:
  1. Prescreening of sustainable aviation fuels (SAF)

Investigation Team

Washington State University

Joshua Heyne (P.I.) Coordinates all team members (both ASCENT and non-ASCENT efforts) and communicated prescreening results with SAF producers.
Zhibin (Harrison) Yang (research assistant professor) Conducts Tier Alpha prediction and Tier Beta measurements.
Conor Faulhaber (PhD student) Conducts seal swell, sulfur, and nitrogen measurements
Patricia Garcia-Alfaro (undergraduate student) Conducts lubricity measurement.

Project Overview

The ASCENT Project 065A focuses on further developing the Tier Alpha and Tier Beta test methods, which can help minimize the fuel volume needed for testing and improve a fuel's potential for meeting ASTM approval criteria. Tier Alpha refers to low-volume analytical testing approaches (i.e., two-dimensional gas chromatography [GCxGC], nuclear magnetic resonance, and infrared analytical testing). Tier Beta tests focus on directly assessing the physical and chemical properties of a fuel rather than predicting properties from GCxGC methods.

Task 1 - Prescreening of Sustainable Aviation Fuels

Washington State University

Objective

The objective of this task is to develop a tiered prescreening process for new alternative jet fuels that uses low fuel volumes and will improve a fuel's potential to meet ASTM approval criteria. This work facilitates the flow of meaningful information to fuel producers when their production processes are at a low technology readiness level while simultaneously strengthening a producer's readiness for the approval process.

Research Approach

Previous annual reports summarized significant progress toward prescreening SAF candidates. The motivation, conceptual application, detailed description, and examples of this effort were described in publications in peer-reviewed journals in the first 18 months of this project. Prior to this report, the ASCENT Project 065A team has reported 18 publications. This report documents four additional peer-reviewed journal articles, published between October 1, 2024, and September 30, 2025. Citations for the articles are listed in the *Publications* section below and are provided as Appendices A-B:

- Paper 19 - "Freezing Point of Hydrocarbon Fuels from Single Species Concentrations" (Bell et al., 2025) in *ACS Energy & Fuels*. (Presented in Appendix A.)
- Paper 20 - "Upgrading of biocrude oil into sustainable aviation fuel using molybdenum carbide nanocatalysts" (Yu et al., 2025) in *Science Advances*. (This is collaboration, where WSU personnel are not the first author)
- Paper 21 - "Measurement of Spray Chamber Ignition Delay and Cetane Numbers for Aviation Turbine Fuels" (Luecke et al., 2025) in *Energy & Fuels*. (This is collaboration, where WSU personnel are not the first author)
- Paper 22 - "Geometric and Positional Isomer Effects on Ignition Behavior of Cycloalkanes: Implications for Sustainable Aviation Fuels" (Yang et al., 2025) in *ACS Energy & Fuels*. (Presented in Appendix B.)

Milestones

- Performed Tier Alpha testing a total of 470 times.
- Performed Tier Beta testing a total of 267 times.
- Determined the maximum blending ratio for 46 SAF candidates.

Major Accomplishments.

- Developed method to predict freezing points from single species concentrations resulting in one publication.
- Measured the derived cetane number in numerous fuels and mixtures resulting in one publication.
- Made many strides on improving aviation fuel blending rules, including a novel blending rule for distillation curves.
- Participated in numerous prescreening collaborations with groups at National Renewable Energy Laboratory (NREL), Massachusetts Institute of Technology (MIT), Pacific Northwest National Laboratory (PNNL), and other groups withing WSU.

Publications

Peer-reviewed Journal Publications

Bell, D. C., Boehm, R. C., & Heyne, J. S. (2025). Freezing Point of Hydrocarbon Fuels from Single Species Concentrations. *Energy and Fuels, 39*(9), 4221-4226. https://doi.org/10.1021/acs.energyfuels.4c06091

Luecke, J., Naser, N., Yang, Z., Heyne, J., & McCormick, R. L. (2025). Measurement of Spray Chamber Ignition Delay and Cetane Numbers for Aviation Turbine Fuels. *ACS Energt & Fuel, 39*(22), 10479-10487. https://doi.org/10.1021/acs.energyfuels.5c01350

Yang, Z., Faulhaber, C., Boehm, R. C., & Heyne, J. S. (2025). Geometric and Positional Isomer Effects on Ignition Behavior of Cycloalkanes: Implications for Sustainable Aviation Fuels. *ACS Energy & Fuel,* 39(38), 18641-18648. https://doi.org/10.1016/j.fuel.2024.133230

Yu, S., He, H., Summers, S., Yang, Z., Si, B., Gao, R., Song, A., Heyne, J. S., Zhang, Y., & Yang, H. (2025). Upgrading biocrude oil into sustainable aviation fuel using zeolite-supported iron-molybdenum carbide nanocatalysts. *Science Advances, 11*(26), 5777. https://doi.org/10.1126/sciadv.adu5777

Outreach Efforts

- Served as panel moderator for Chief Executive Officer (CEO) and Co-founder of Volaris, CEO and Founder of CleanJoule, Chief Sustainability Officer of Pratt & Whitney, and US SAF Ambassador (2025, July) for "Expansion and Security of Aviation Fuel Availability Globally," AIAA ASCEND, Las Vegas, Nevada. Sponsored travel.
- Presented at and participated in multiple relevant meetings, panels, and conferences.

Presentations

Heyne, G. (2024, September). *SAF Center at Paine Field* [Panel presentation]. 19th Annual Aerospace Summit, Aerospace Futures Alliance, Tacoma, Washington.

Heyne, G. (2024, September 16). Drop-in solutions to minimize aviation fuel sooting. International Civil Aviation Organization (ICAO) Symposium on non-CO_2 Aviation Emissions, Montréal, Canada. Sponsored travel.

Heyne, G. (2024, October). *Collaborating to Decarbonize Aviation* [Panel presentation]. Ohio State Sustainable Aviation Forum, Ohio State University – Columbus, Center of Aviation Studies. Sponsored travel.
Heyne, G. (2024, December). *Contrail Avoidance and Mitigation with Fuel Composition* [Meeting presentation]. Rocky Mountain Institute (RMI), Contrail Impact Task Force Meeting.
Heyne, G. (2025, August). *ART OF THE POSSIBLE: Shaping Cutting-Edge Economic Opportunity for Washington's Future!* [Panel presentation]. Washington Economic Development Association, Tacoma, Washington.

Awards

None

Student Involvement

- Conor Faulhaber (PhD student) has made many of the measurements discussed herein and commissioned some the test methods used.
- Patricia Garcia-Alfaro (undergraduate student) has contributed to the measurements discussed herein.

Plans for Next Period

- Expand testing to include numerous new testing equipment. These include combustion ion chromatography, coupled plasma–optical emission spectroscopy (ICP-OES), graphite furnace, and more.
- Publish trace polar molecules impact on lubricity in alternative jet fuel.
- Continue to develop our O-ring swell measurements to test the effects of low temperature on O-ring swell. This is in addition to the work we perform for fuel producers through Tier Alpha and Tier Beta.

APPENDIX A

Freezing Point of Hydrocarbon Fuels from Single Species Concentrations

Bell, D. C., Boehm, R. C., & Heyne, J. S. (2025). Freezing Point of Hydrocarbon Fuels from Single Species Concentrations. *Energy and Fuels, 39*(9), 4221-4226. https://doi.org/10.1021/acs.energyfuels.4c06091

Introduction

The freeze point of a petroleum-refined fuel has traditionally been regarded as a difficult property to predict with confidence. These challenges are amplified when applied to synthetic fuels. One of numerous factors contributing to this is that freezing point is very sensitive to hydrocarbon structure [1]. For example, 2-methylheptane has a freezing point below the measurement limit of the PAC 70Xi freezing point machine used in this experiment (<-88 °C) while a different C8H18 isomer, 2,2,3,3-tetramethylbutane is a solid at room temperature. This difference between their freeze points that is only attributable to structure makes methods relating hydrocarbon group type compositions to the bulk mixture freezing point unreliable. Compositional relationships from the literature have used n-alkane concentration, aromatic concentration, and distillation curve information among other properties to try to predict the freezing point, but these methods designed around petroleum-refined fuels have been ineffective when applied to alternative fuels [2,3]. Such fuels generally have similar ratios of isomers within groups, even as the group concentrations vary. Petroleum-refined fuels generally have 'smooth' carbon number distributions peaking at C11 or C12. They are primarily mixtures of n-alkanes, iso-alkanes, cyclo-alkanes, and alkyl-benzenes, made up of over 1000 different species. The specific species with the highest concentrations are almost always n-alkanes. N-Alkanes, especially high carbon number n-alkanes, have been identified qualitatively as the cause for high freezing point fuels, but this has not been translated into specific predictions [4–6].

For alternative fuels, the fuel composition can be dramatically different. For instance, many fuels are comprised of a single hydrocarbon family. Hydroprocessed Esters and Fatty Acids (HEFA) is primarily alkanes; Cycloparaffinic Kerosene (CPK-0), which is currently in the ASTM D4054 process, is composed of cycloalkanes; Synthetic Aromatic Kerosene (SAK) is only aromatics. Alternative fuels do not always have many species. Farnesane, the product of ASTM D7566 Annex A3, is composed of only one species, 2,6,10-trimethyldodecane. Iso-butanol-to-jet procedures effectively only produce two species in major quantities, 2,2,4,6,6-pentamethylheptane and 2,2,4,4,6,8,8-heptamethylnonane. These types of products necessitate a freeze point prediction model which can handle major differences in composition. In this work, we seek to develop a practical model based around the fundamental physics of freezing and mixing.

In 2022, Boehm et al. published a paper proposing a thermodynamically derived method of predicting the freezing point of a mixture [7]. One of the primary conclusions of this work is that freezing point is determined by the concentration of a single controlling species and the balance of the sample negligibly affects the freeze point. This results in another challenge observed in predicting the freezing point, that the blending rule is not linear because the relationship between freeze point and concentration is not linear and because the controlling species may differ from one fuel to another. The published empirical blending rules for freeze point prediction of blends of petroleum-refined fuels are not effective for blends of dissimilar solutions. This will be demonstrated in more detail in this paper. Alternatively, the experimental scope of Boehm et al. was limited to mixtures having a concentration of the freezing component greater than 10% by mole. Such concentrations are higher than any individual hydrocarbon in conventional jet fuel. Moreover, and in spite of being significantly simpler than a prior thermodynamically-derived model, [8] that model requires several thermodynamic property inputs such as enthalpy and entropy of fusion as well as liquid and solid phase heat capacities, which are not always readily available. Such absence of inputs makes it difficult to implement in fuel-property prediction models. Adding to this inconvenience, the Boehm model is an implicit function T=f(T,x) for which an iterative solution methodology is not always well-behaved.

Although the thermodynamic models [7,8] are impractical for complex fuel predictions, the fundamentals behind them are tractable for a simpler model. Boehm's model suggests that freezing point of a fuel is limited by the freezing point of only one molecule which implies we only need to identify and characterize that one species to get a freezing point prediction. For a given complex fuel sample, we only need to characterize the concentrations of species with high freezing points and we can apply the model to each of these species and logically select the maximum value from this set of interim predictions. Taking this a step further, we do not need to use a thermodynamic model at all to predict values. Because the

balance of the hydrocarbons in the mixture was deemed unimportant, the freeze point of species k, as a function of concentration of this species can be measured experimentally in blends with control hydrocarbons, and the resulting control curves can be used in place of the moderately complex thermodynamic model to explicitly relate freeze point of species k to its concentration in the mixture. GC×GC/FID-VUV is perfectly suited for determining concentration of individual species in complex mixtures [9]. All specific isomers with relatively large concentrations that have been seen before are included in the spectral database and will continue to grow as more species relevant to freeze point are identified.

In this work, we explore the above hypothesis expanding upon the work of Boehm et al. [7] to improve the scientific understanding of the impact of composition on freezing point. We will detail the problems associated with other freezing point models, evaluate the experimental control curve as a prediction method, and determine the accuracy of the conclusions made in Boehm et al. First, we present additional results reinforcing the theory of Boehm et al. by showing the freezing point of blends of two high freezing point species (n-tridecane and bicyclohexyl) result in a decrease in freezing point, a trait which will not be predicted in most other models. Next, we test C11-C17 n-alkanes in iso-octane to generate reference data predicting when each of these species will freeze in a mixture at various concentrations. We use these data to test the hypothesis when applied to synthetic fuels. Then, we perform tests to isolate the 2nd order effects of species interaction and blending. Finally, we leverage the results of this research to generate a 100% n-alkane fuel that passes the ASTM D1655 limit for freeze point.

Method

Principal Component Quantitation

Freezing point measurements of many hydrocarbon blends are discussed. Freezing point is measured using a Phase Technology PAC 70Xi: Cloud, Pour, and Freeze Point Analyzer, following the procedure described in ASTM D5972. The machine has a reporting resolution of 0.1 °C and can measure between -88 °C and 70 °C. 0.15 mL samples are injected into a metallic sample chamber with a reflective bottom surface which is used for reflecting light to measure diffusive light scattering. When an experiment is started, the temperature is decreased in the chamber at a rate of 15 ± 5 °C/min until the detected opacity exceeds a threshold suggesting that the sample is mostly solid. The system then begins to increase the temperature at a rate of 10 ± 0.5 °C/min. Freezing point, or more accurately melting point, is determined when the opacity returns to the original flat line observed while cooling. According to the Phase Technology product brochure, the rated reproducibility is ±0.8 °C.

In this work, tests are performed on complex fuel samples, single components, and mixtures. The complex fuel mixtures used in this work are all 'prescreening fuels' from the FAA ASCENT project 65a. The fuels are sourced from numerous fuel producers, national labs, and universities and include many different conversion pathways including hydrothermal liquefaction (HTL), HEFA, and alcohol-to-jet (ATJ). For mixtures, blending was performed by mass and converted to moles, accordingly. Most of the mixtures are using pure components where molecular weight is provided; for synthetic aromatic kerosene (SAK), the molecular weight is calculated from GCxGC data [9]. For the complex fuels, mole concentrations are measured using GCxGC-MS/FID performed by colleagues at University of Dayton Research Institute [10,11].

Results

Freezing Point Blend Rule Non-Linearity

For many applications, blending rules are desired for fuel properties. For many properties, a straight-forward scalar product between a concentration vector and a properties vector is sufficiently accurate for developing synthetic fuel assessments. The freezing point blend rule that was originally adopted by Yang et al. [12] for Tier α fuel pre-screening came from the work of Al Mulla et al. [3] (presented as the green line in Figure A-1) which utilizes a logarithmic transformation, but generally mimics a linear by volume blending rule. (Those authors claim a mean absolute error of 0.05 K for this model, but we are skeptical of this value.) The model fundamentally suggests that the addition of species with a higher freezing point than the starting mixture will increase the freezing point and vice versa. This concept strictly competes with the hypothesis of Boehm et al. This model was developed using results from blends of petroleum-based fuels. In petroleum fuels, the freezing component is almost certainly an n-alkane that is present in both mixtures. When the component that is determining the freezing point is not in both samples the model falls apart.

Boehm et al. utilized blends of relatively large concentrations (>10%) of high freezing point components (n-tridecane and bicyclohexyl) in complex fuels to support the theoretical assertions. These mixtures demonstrated that the fuel into which the freezing component is blended has little effect on the freezing point. However, in these tests, it was known that a high

freezing point component was being added to a mixture that was not expected to freeze. This work did not demonstrate the assertion that a mixture of two different solutions whose freeze points are controlled by different species can, when blended, result in a mixture with a lower freeze point than either of the preblended solutions. In Figure A-1, the freezing points of mixtures of bicyclohexyl in n-tridecane (gold line) are compared against the freezing points of bicyclohexyl (red line) and n-tridecane (blue line) in a solvent that we know will not freeze, iso-octane (2,2,4-trimethylpentane, freezing point = ~-110 ˚C). The freezing points of the neat hydrocarbons used in this work are included in Table A-1. The first observation is the difference between the green line representing the Al Mulla blending model prediction of the freezing point of the bicyclohexyl/tridecane blends compared to the experimental results of these blends. The freezing point of the blend is consistently lower than the prediction. Now, compare the experimental results of the tridecane/bicyclohexyl blends to the components individually blended in iso-octane. The freezing point of the blends closely track the greater of the blue and red lines. There is a bimodal response consistent with the hypothesis of Boehm et al.[7]. This plot emphasizes the issues with the Al Mulla blending rule and demonstrates the potential for a new method.

Table A-1. Freezing points of the pure hydrocarbons used in this study.

Name	Freeze Point, ˚C
nC8	-58
nC11	-25.5
nC12	-9.5
nC13	-5.3
nC14	5.8
nC15	9.9
nC16	18.1
nC17	21.9
Iso-octane	-108
bicyclohexyl	7.5

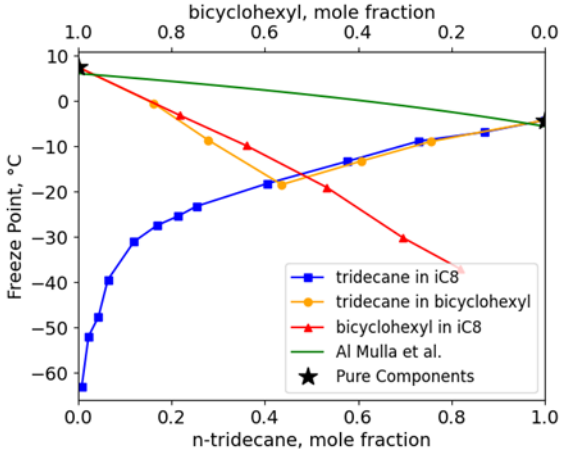

Figure A-1. Tridecane and bicyclohexyl blends are measured for freezing point and compared to the old freezing point blend rule. Additionally, 'control curves' of bicyclohexyl and tridecane in iso-octane are included to demonstrate that the freezing point of a tridecane limited mixture is the same whether it is blended in a high freezing point substance (bicyclohexyl) or a non-freezing component (iso-octane).

Data Driven Control Curve Model

n-Alkanes are known for their high freezing points and are often blamed when a fuel has a poor freezing point. This is supported by the numerous models correlating n-alkane concentration to freezing point [2,6]. Additionally, n-alkanes are typically the highest concentration single species in petroleum-refined fuels. The combination of them being high freezing point species and frequently in relatively high concentrations justify their selection as species to highlight during fuel screening. They are the focus of this research, but additional species could be included in a similar manner.

Equations A-1 – A-3 are the thermodynamically derived equations of Boehm et al.

$$T_{f,mix} = \max\left(T_{f,mix,i}(x_i, i)\right) \quad \text{(Eq. A-1)}$$

$$T_{f,mix,i} = \frac{\Delta H_{fusion,i} + x_i \times (Cp_{sol,i} - Cp_{liq,i}) \times (T_{f,i} - T_{f,mix,i})}{\Delta S_{fusion,i} + x_i \times (Cp_{sol,i} - Cp_{liq,i}) \times ln\left(\frac{T_{f,i}}{T_{f,mix,i}}\right) + \alpha \times \Delta S_{mixing}} \quad \text{(Eq. A-2)}$$

$$\Delta S_{mixing} = -R \times \frac{1}{X_j} \times \left[(1 - X_j) \times ln(1 - X_j) + X_j \times ln(X_j)\right] \quad \text{(Eq. A-3)}$$

Where T_f is freezing point temperature, 'x' is for mole fraction, subscript 'i' is for various species, H is enthalpy, S is entropy, Cp is heat capacity, and R is the ideal gas constant.

In this work, we suggest the replacement of Equations A-2 and A-3 with tabulated experimental results of species in a non-freezing solution (iso-octane). To execute this, we gather data for the freezing point of n-alkanes from n-undecane (C11) to n-heptadecane (C17) in a range of concentrations in iso-octane. The reported lines serve as control curves and represent when the various molar concentrations of these species will freeze in a more complex mixture. These control curves are plotted in Figure A-2. In Figure A-2, it is seen that the freezing point is linear with concentration on log scale. This feature allows for interpolation of the best fit line to determine the freezing point caused by a given species. One noteworthy result from this figure is that at a mole concentration of 0.2% n-hexadecane in iso-octane will fail the -40 ˚C specification limit for freezing point. This exemplifies why mixtures with n-alkanes, especially when associated with higher molecular weight, can have difficulty passing freezing point; very small quantities of n-hexadecane can have a major influence on freezing point. Another interesting observation is the similarity in the freezing point curves between even/odd pairs of n-alkanes (e.g., nC14 and nC15).

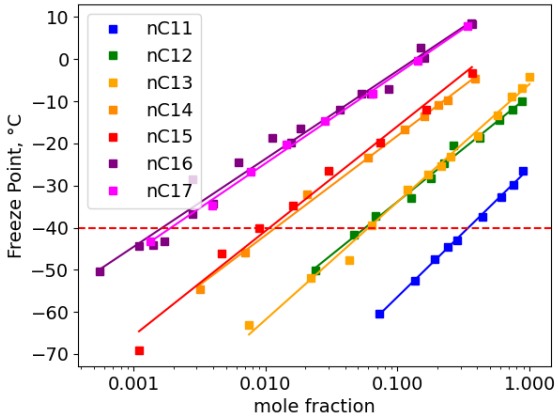

Figure A-2. Freezing point of various n-alkanes blended in a non-freezing control solvent (iso-octane). At a given concentration for any of these n-alkanes in a fuel, the point at which it will freeze in a fuel can be determined by interpolating between the reported data.

Freezing Point Prediction Accuracy

The freezing point of twenty-four sustainable aviation fuel candidates are predicted using the method described above. For consistency, all of the compositional information comes from GCxGC testing done by the University of Dayton Research Institute. The freezing point values were measured within the lab at Washington State University. The sustainable aviation fuel candidates are very diverse coming from various research pathways. Using the iso-octane control curves from Figure A-2 as the prediction, Figure A-3 shows the parity plot of the predicted and measured freezing points. The unity line is shown in black, and the best fit line is shown in blue. Interestingly, none of the predictions are lower than the measurement. This hints that blending with iso-octane represents an upper limit of the freeze point, which is counterintuitive. In these examples the lower freeze point 'solvent' results in a higher freezing point mixture, given the same concentration of the high-freeze-point solute. The predictions generally capture the trend well, but there is a consistent offset of about 12 ˚C. The best fit line is approximately horizontal to the unity line (slope=0.988). In addition to the freeze point experimental uncertainty, the greatest potential source of error is the quantification of the n-alkane concentrations. This prediction method is sensitive to slight changes in the limiting high-molecular-weight n-alkane concentration. There could also be errors associated with the measurement of the control curves which would propagate into these predictions as well. Moreover, it is entirely possible that the 12 ˚C offset is not indicative of an error with any of the model inputs, but rather with the assumption that the solvent characteristics such as the number of components, hydrocarbon types, density, or the presence of other solutes that may freeze at nearly the same temperature do not matter. In the next section we explore this question in more detail.

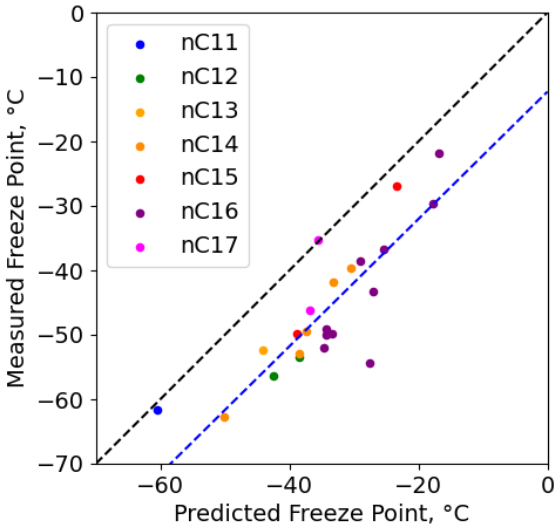

Figure A-3. Parity plot of predicted freezing points using the control curve approach compared to measured freezing points. The unity line is included in black, and a best fit line is included in blue. All of the predictions are higher than the measured freezing points.

Second Order Effects on Freezing Point

In Figure A-3, we see that the freezing point of specific species in a mixture is often lower than the freezing point of the same species in iso-octane. Affens et al. [13] observed that in ternary mixtures of n-tridecane, n-hexadecane and Isopar 150 (an isoparaffinic solvent), the freezing point at times decreased when both n-hexadecane and n-tridecane were present. These results were recreated in our lab using iso-octane in place of Isopar 150 with similar results, albeit to a lesser magnitude. The current results are shown in Figure A-4. These results suggest that the identity of components other than the first solute to freeze may have some impact on the freezing point of the solute. In this example, normal alkanes other hexadecane can depress the freeze point of hexadecane, from a 0.17% solution of hexadecane, by up to 12 ˚C depending on how much of the companion normal alkanes are present. However, the presence of a different solute (bicyclohexyl) that is predicted to freeze out of solution at nearly the same temperature as hexadecane is shown to have little impact on the freeze point of hexadecane.

Returning to the assumptions that fed into the simplified theory that is represented by Equation A-2, there are two convenient hypotheses to potentially explain the presence of a second order effect. One is that the entropy of mixing term may vary based on similarity of the solute with the remainder of the solution. The other is that of incomplete separation of molecular species between phases; meaning that perhaps the solid phase is not 100% hexadecane, but rather some solid-state, molecular-level mixture that is mostly hexadecane but partially n-tridecane and n-octane. Regardless of its cause, the magnitude of this second-order effect seems to plateau at 12 ˚C for 0.17% hexadecane solutions.

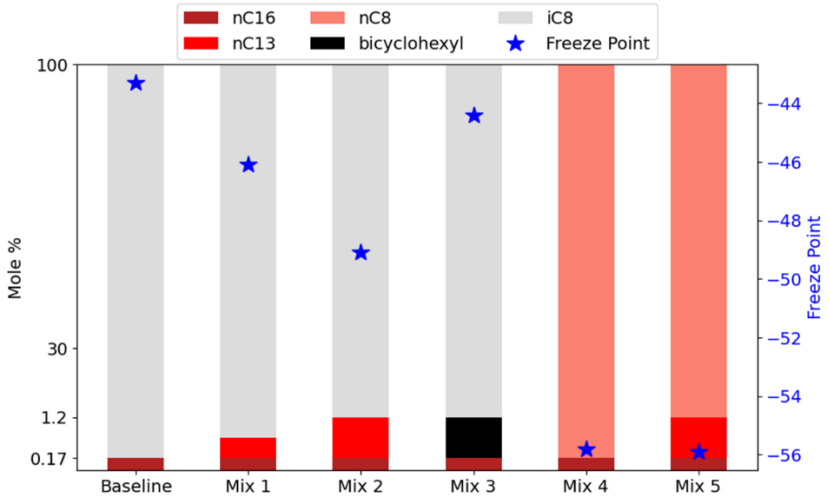

Figure A-4. Freezing points of 0.17% hexadecane in various mixtures. Composition is described by the color of the bar. NOTE: the sizes are not drawn to scale. The freezing point of each mixture is noted with the blue star. The baseline and mixtures 1 and 2 recreate the results of Affens et al.

We expanded on this analysis by exploring how different solutions impact the freezing point of the limiting component. Figure A-5 shows the freezing point of n-hexadecane when blended at various proportions into a variety of solvents. In each case the freezing point of hexadecane is linear with the log of its molar concentration. The highest of these curves is what we refer to as the first order effect, as we assume ethylbenzene has negligible impact on the purity of the freezing hexadecane and provides a bounding example for the entropy of mixing term (the α scalar) in Equation A-2. The magnitude of second order effect is the difference between the top (black, ethylbenzene) curve and any other curve. In this example, methylcyclohexane, dimethylcyclohexane, n-octane, SAK, and mixture of dodecane isomers each produce a second order effect with approximately the same magnitude, which is approximately 30% that of the first order effect, regardless of the hexadecane (solute) concentration. Pragmatically, the significance here is that both of these effects are always negative. Note: The reference solvent that is chosen to represent the first order effect may not always be truly bounding; however there is significant anecdotal evidence to suggest that complex solvents (such as jet fuels) will never have a less negative second order effect than any reasonably chosen reference solvent; a single-component hydrocarbon, dissimilar in size and type from the solute.

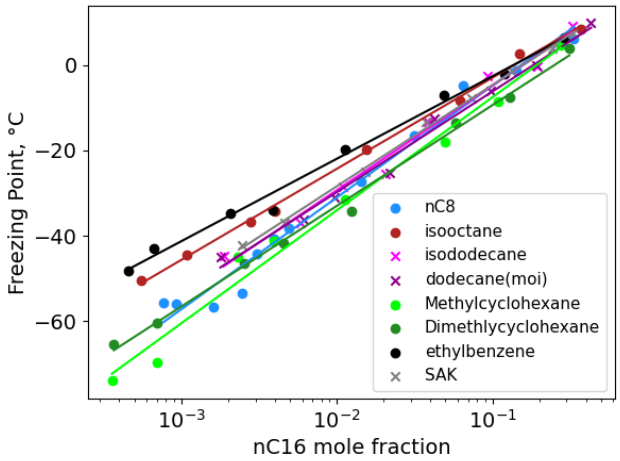

Figure A-5. Freezing point of n-hexadecane in various solvents. Solvents containing only one species are marked with circles and mixtures are marked with 'x's. n-Alkane and cycloalkane solvents result in a lower freeze point of nC16 than aromatic or iso-alkane solvents. The three complex mixtures (two different sets of mixtures of isomers of dodecane and Synthetic Aromatic Kerosene [SAK]) all resulted in very similar curves. The 'moi' after dodecane stands for 'mixture of isomers.'

100% n-Alkane Fuel

Fuels with large concentrations of n-alkanes are generally associated with higher freezing points. Eight of the nine models included in Wang et al.'s review of freezing point included concentration of n-alkanes as factors positively correlated with freezing point [2]. To reinforce one of the critical implications of this method that freezing point is not determined by group concentrations or bulk property characteristics, we created a 100% n-alkane fuel with comparable molecular weight to Jet A with a freezing point below the Jet A specification (-40 ˚C). This fuel is designed such that every n-alkane starting from nC16 and descending has approximately the concentration which would cause that species to freeze out in a mixture. The mole concentrations of the fuel blended are included in Table A-2. At these concentrations, all of the species between nC10 and nC16 would be expected to freeze in a solvent at approximately the same temperature (-40 ˚C). This mixture has an average molecular weight of 145 g/mol and has an ASTM D2887 simulated distillation curve shown in Figure A-6. This mixture was designed to emphasize the weaknesses of the empirical models based on petroleum-derived samples. Out of the 9 models shared in Wang et al., the closest prediction for the freezing point of this fuel is -12.7 ˚C; the measured freezing point is -40.7 ˚C. The model suggested here predicts -44.1 ˚C. Correlative methods fail to capture the physics which are controlling the freezing point which results in large errors when predicting the freezing point of fuels that are significantly different from those used in creating the model.

Table A-2. Mole percentages blended for the 100% n-alkane used in Figure A-6.

Molecule	Mole %
nC16	0.13%
nC15	0.91%
nC14	0.86%
nC13	4.40%
nC12	4.57%
nC11	25.71%
nC10	25.89%
nC9	37.52%

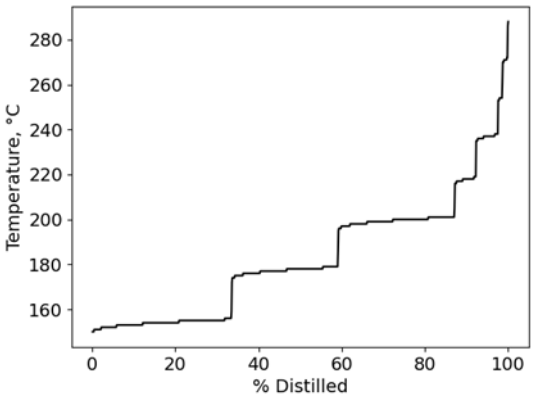

Figure A-6. ASTM D2887 Distillation Curve of a 100% n-alkane fuel.

Discussion

Aviation fuel freezing is primarily determined by the freeze point of a single component. Reducing the concentration of that component will lower the freezing point of the mixture unless another component begins to dominate freezing behavior. To a first order, this phenomenon can be predicted by accurately measuring the concentration of all plausibly limiting solutes in a given sample of an arbitrary hydrocarbon mixture. In petroleum-refined fuels, the limiting species is typically an n-alkane. These species are in high concentrations in petroleum and have high freezing points. Quantities as low as 0.5% of n-hexadecane can cause the fuel to be outside of the acceptable freeze point range for jet fuel regardless of the contents of the remainder of the fuel. For alternative fuels with more diverse and unique compositions, the n-alkanes will not always be the freeze-controlling species. Many alternative fuel candidates contain high concentrations of a single component. For these fuels, the structure of the most prevalent species will be important. Any species that shows up as a plausible freeze point controlling component can be identified using analytical chemistry approaches, including GC×GC-VUV. If not already available, this structural isomer identification would be augmented by the creation of new control curves specific to each of the plausible limiting isomers. Once those data are generated, the specific offending species can be identified and targeted for concentration reduction in future synthetic pathways.

Many species in petroleum-refined jet fuel, if isolated, would have a freezing point higher than the -40 ˚C limit (for Jet A) set in ASTM D1655. The same is true of synthetic blend components (SBC). Individually, the SBC must adhere to the requirements detailed in the annexes of ASTM D7566. The upper limit on the freezing point of SBC is also -40 ˚C which is overly restrictive unless the freezing point of the SBC happens to be governed by a high molecular weight, normal alkane, which is not the case for any of the eight synthetic pathways approved thus far. The results of this work suggest that the freezing point of all SBC/petroleum blends will be less than the freezing point of either one prior to mixing, and that limit for SBC should be applicable a blend of the SBC at its maximum allowed concentration with some reference solvent. However, a note of caution should be added, stating that a higher freezing point may be observed for SBC/petroleum blends if the petroleum component happens to contain a significant concentration of the same molecule that is controlling the freezing point of the neat SBC. Ultimately, the freezing point limit that is specified in ASTM D7566 Table 1 shall control the SBC/petroleum blend.

References

[1] Hall, C., Bell, D. C., Feldhausen, J., Rauch, B., & Heyne, J. (2024). Quantifying isomeric effects : A key factor in aviation fuel assessment and design. *Fuel, 357*,129912. https://doi.org/10.1016/j.fuel.2023.129912

[2] Wang, X., Jia, T., Pan, L., =Liu, Q., Fang, Y., Zou, J. J., & Zhang, X. (2021). Review on the Relationship Between Liquid Aerospace Fuel Composition and Their Physicochemical Properties. *Trans. Tianjin Univ., 27*, 87–109. https://doi.org/10.1007/s12209-020-00273-5

[3] Al Mulla, H.A., & Albahri, T. A. (2017). Predicting the properties of petroleum blends. *Pet. Sci. Technol., 35*, 775–782. https://doi.org/10.1080/10916466.2016.1277238

[4] Ervin, J. S., Zabarnick, S., Binns, E., Dieterle, G., Davis, D., & Obringer, C. (1999). Investigation of the use of JP-8+100 with cold flow enhancer additives as a low-cost replacement for JPTS. E*nergy and Fuels, 13*, 1246–1251. https://doi.org/10.1021/ef9901600

[5] Van Winkle, T. L., Affens, W. A., Beal, E. J., Mushrush, G. W., Hazlett, R. N., & Deguzman, J. (1987). Determination of liquid and solid phase composition in partially frozen middle distillate fuels. *Fuel, 66,* 890–896.

[6] Striebich, R. C., Motsinger, M. A., Rauch, M. E., Zabarnick, S., & Dewitt, M. (2005). Estimation of select specification tests for aviation turbine fuels using fast gas chromatography (GC). *Energy and Fuels, 19*, 2445–2454. https://doi.org/10.1021/ef050136o

[7] Boehm, R. C., Coburn, A. A., Yang, Z., Wanstall, C. T., & Heyne, J. S. (2022). Blend Prediction Model for the Freeze Point of Jet Fuel Range Hydrocarbons. *Energy & Fuels*. https://doi.org/10.1021/acs.energyfuels.2c0206

[8] Coutinho, J. A. P., Andersen, S. I., & Stenby, E. H. (1995). Evaluation of activity coefficient models in prediction of alkane solid-liquid equilibria. *Fluid Phase Equilib., 103*, 23–39. https://doi.org/10.1016/0378-3812(94)02600-6

[9] Feldhausen, J., Bell, D. C., Yang, Z., Faulhaber, C., Boehm, R., & Heyne, J. (2022). Synthetic aromatic kerosene property prediction improvements with isomer specific characterization via GCxGC and vacuum ultraviolet spectroscopy. *Fuel, 326*, 125002. https://doi.org/10.1016/j.fuel.2022.125002

[10] Johnson, K., Loegel, T., Metz, A., Wrzesinski, P., Shafer, L., Striebich, R., & West, Z. (2020). *Method for Detailed Hydrocarbon Analysis of Middle Distillate Fuels by Two-Dimensional Gas Chromatography*. NAVAIR Public Release 2020-361.

[11] Striebich, R. C., Shafer, L. M., Adams, R. K., West, Z. J., DeWitt, M. J., & Zabarnick, S. (2014). Hydrocarbon group-type analysis of petroleum-derived and synthetic fuels using two-dimensional gas chromatography. *Energy and Fuels, 28*, 5696–5706. https://doi.org/10.1021/ef500813x

[12] Yang, Z., Kosir, S., Stachler, R., Shafer, L., Anderson, C., & Heyne, J. S. (2021). A GC × GC Tier α combustor operability prescreening method for sustainable aviation fuel candidates. *Fuel, 292*, 1–9. https://doi.org/10.1016/j.fuel.2021.120345

[13] Affens, W. A., Hall, J. M., Holt, S., & Hazlett, R. N. (1984). Effect of composition on freezing points of model hydrocarbon fuels. *Fuel, 63*, 543–547. https://doi.org/10.1016/0016-2361(84)90294-1

APPENDIX B

Geometric and Positional Isomer Effects on Ignition Behavior of Cycloalkanes: Implications for Sustainable Aviation Fuels

Yang, Z., Faulhaber, C., Boehm, R. C., & Heyne, J. S. (2025). Geometric and Positional Isomer Effects on Ignition Behavior of Cycloalkanes: Implications for Sustainable Aviation Fuels. *ACS Energy & Fuel, 39*(38), 18641-18648. https://doi.org/10.1016/j.fuel.2024.133230

Introduction

The commercial aviation industry is facing mounting pressure to reduce greenhouse gas (GHG) emissions. In the United States, the Sustainable Aviation Fuel Grand Challenge has set ambitious goals: a 50% reduction in aviation-related GHG emissions and full substitution of fossil-based jet fuel with Sustainable Aviation Fuel (SAF) by 2050[1]. Similarly, the ReFuelEU Aviation Regulation mandates that SAF comprise at least 2% of jet fuel at EU airports by 2025, rising to 70% by 2050[2]. Achieving these targets requires not only scale-up of existing production but also the approval of new SAF production pathways. However, most currently certified ASTM D7566 pathways (e.g., A2 HEFA, A5 ATJ) primarily yield synthetic paraffinic kerosene (SPK), which consists almost entirely of n- and iso-alkanes. Although some pathways (e.g., A6 CHJ, A8 ATJ-SKA) can produce aromatic and cycloalkane components, their commercial-scale output remains limited.

There is growing interest in SAF candidates derived from novel feedstocks and conversion technologies, particularly those that produce predominantly aromatic and cycloalkane-rich fuels. Many of these are progressing through the ASTM D4054 approval process. However, due to limited research and historical uncertainty regarding cycloalkane behavior in combustion, original equipment manufacturers (OEMs) and regulatory bodies continue to limit the cycloalkane content within certain D7566 annexes and specifications. One key distinction between cycloalkanes and other hydrocarbon classes found in jet fuel (e.g., n- and iso-alkanes, aromatics) is the presence of cis-trans isomerism, also known as geometric isomerism. Although alkenes also exhibit geometric isomerism, their poor thermal stability renders them present only in trace amounts in conventional jet fuels and absent from all currently approved SAFs.

Ignition delay (ID) and derived cetane number (DCN) are key metrics used to characterize the combustion reactivity of liquid fuels[3,4]. Ignition delay is defined as the time between the start of fuel injection and the onset of significant combustion. DCN, a dimensionless quantity, is inversely related to ignition delay and serves as a standardized indicator of ignition quality. For aviation turbine fuels, maintaining DCN in the range of 35 to 60 is critical to ensure safe and efficient engine operation[5]. Fuels with excessively low DCN (i.e., long ignition delay) may increase the risk of lean blowout (LBO), particularly under high-altitude or low-load conditions[6]. Conversely, fuels with excessively high DCN (i.e., short ignition delay) may contribute to hardware durability issues, especially upstream of the primary reaction zone where large heat release is not anticipated by the hardware designers. As a result, understanding and controlling ignition delay behavior is essential for SAF certification and performance optimization.

The ignition behavior of hydrocarbons is strongly influenced by their molecular structure, particularly in the case of cyclic and branched alkanes. Cycloalkanes like DMCH are of growing interest in SAF formulations and surrogate development due to their abundance in lignin-derived fuels[7,8]. Dimethylcyclohexane (DMCH), with its multiple positional and geometric isomers, offers an ideal molecular platform to examine the structural sensitivity of fuel reactivity. However, their behavior during autoignition differs substantially from linear or branched alkanes. The cis-trans configuration, resulting from the rigid ring structure, modulates steric strain, radical stability, and low-temperature reaction pathways. For instance, cis-isomers tend to ignite more readily than trans-isomers, owing to reduced conformational strain and more favorable intramolecular hydrogen shift (1,5-H shift) mechanisms[9]. This trend is consistent across several cycloalkane systems, including decalin, where Heyne et al.[10] reported a significantly higher derived cetane number (DCN ≈ 41.6) for cis-decalin than trans-decalin (DCN ≈ 32.0) under identical IQT conditions. This trend is further supported by detailed structural and experimental analysis of decalin. Decalin exists as a fused bicyclic cycloalkane with two ring junction configurations: cis-decalin, where both hydrogens at the ring junctions are on the same face, and trans-decalin, where they are on opposite faces. The cis isomer adopts a more flexible conformation, which allows for enhanced low-temperature reactivity due to more favorable hydrogen abstraction and chain-branching pathways. In contrast, the trans isomer exhibits a more rigid structure with lower reactivity under similar conditions.

Beyond geometry, positional isomerism also plays an important role. Prior studies report that 1,2-DMCH exhibits significantly lower reactivity than 1,3-DMCH, attributed to steric hindrance around the methyl groups and fewer accessible β-scission pathways[11]. Experimental work by Kang et al.[12] and Yang & Wang[13] supports this trend, demonstrating that 1,3-isomers produce earlier low-temperature heat release and higher radical concentrations in motored engine studies and quantum kinetic calculations.

These structural effects are also reflected in DCN measurements. Using IQT, Jameel et al.[14] measured a DCN of 24 for 1,2-DMCH and 30.5 for 1,3-DMCH, supporting the view that increased substitution near the ring reduces reactivity. However, their study did not provide detailed characterization of isomer purity or cis-trans ratios, limiting interpretation of configurational effects. Similarly, Do et al.[15] investigated ring-opening reactions of 1,2- and 1,3-DMCH over iridium-based catalysts and predicted cetane numbers using artificial neural networks, obtaining CN = 22 for 1,2-DMCH and CN = 30 for 1,3-DMCH. These predicted and experimental values align well with the trend that increased substitution near the ring reduces reactivity, but also highlight the sensitivity of these metrics to both position and geometry of substituents.

A recent comprehensive study by Yang et al.[16] provided direct comparative insight into the oxidation kinetics of 1,2- and 1,3-DMCH using flow reactor experiments and detailed chemical kinetic modeling. Their work revealed that 1,2-DMCH exhibits stronger high-temperature reactivity, whereas 1,3-DMCH is more reactive under low-temperature conditions, particularly within the negative temperature coefficient (NTC) regime. Their study contributed validated kinetic sub-models for both isomers, yet did not differentiate cis- and trans- configurations, highlighting a critical gap in understanding the role of geometric isomerism in ignition behavior.

Other modeling efforts, such as those by Kubic[9], used group contribution methods and neural networks to predict DCNs across a wide molecular domain. These models confirmed that ring substitution, branching, and unsaturation consistently reduce cetane numbers, primarily through their inhibitory effects on early-stage radical formation and propagation. Additionally, Rosado-Reyes and Tsang[17] explored the isomerization kinetics of cis-1,2-DMCH in a single-pulse shock tube. Their findings showed unexpectedly slow cis-to-trans isomerization, suggesting kinetic bottlenecks due to steric hindrance in cyclic transition states.

Collectively, these findings emphasize the necessity of treating geometric and positional isomers as discrete species in kinetic models. Their differences are not merely of academic interest but bear significant implications for SAF performance metrics such as ignition delay, lean blowout risk, and nvPM emissions[18]. Despite growing understanding of DMCH oxidation chemistry, there remains a lack of experimental data that clearly isolates geometric isomerism effects under tightly controlled conditions. Many previous studies either used mixed isomer samples or did not specify isomeric purity, limiting mechanistic conclusions. As a result, detailed characterization of ignition delay and DCN as a function of cis-trans configuration remains an open research question.

In this work, we present a systematic investigation of the effect of geometric isomerism specifically cis vs. trans configurations—on the ignition delay of high-purity dimethylcyclohexane and decalin isomers. This study aims to fill a critical knowledge gap in surrogate fuel modeling and contribute to the broader understanding of how molecular structure dictates fuel performance in advanced combustion systems.

Materials and Methods

Reference Materials

All six configurations of DMCH and their mixtures were purchased for testing as shown in Table B-1. Some configurations of fuel were purchased twice to acquire different lot numbers and used for cross referencing.

Table B-1. Hydrocarbons used in this study, including source and purity.

Molecules	Purity	Lot number	Company
cis-1,2-dimethylcyclohexane	>98%	FIJ01-KU	TCI America
trans-1,2-dimethylcyclohexane	>99%	KRFHJ-QI	TCI America
cis-1,2-dimethylcyclohexane	>98%	FHA01-BN	TCI America
trans-1,2-dimethylcyclohexane	>99%	KRFHJ-BQ	TCI America
cis-1,3-dimethylcyclohexane	>99%	FB001-OX	TCI America
trans-1,3-dimethylcyclohexane	>95%	HD6TH-CM	TCI America
trans-1,3-dimethylcyclohexane	>98%	HD6TH-OK	TCI America
cis-1,4-dimethylcyclohexane	>98%	FHC01-NOJD	TCI America
trans-1,4-dimethylcyclohexane	>95%	G3HHM-US	TCI America
trans-1,4-dimethylcyclohexane	>95%	X7YKC-TT	TCI America
cis-decalin	>98%	TED3A-SN	TCI America
trans-decalin	>98%	7SQEF-LB	TCI America

Sample Preparation

As with any hydrocarbon-based fuel, prolonged exposure to atmospheric oxygen can lead to the formation of trace oxygenates and peroxides. These oxidative degradation products can significantly affect ignition delay measurements by altering fuel reactivity. To minimize these effects and ensure consistent sample quality, solid phase extraction (SPE) was employed to remove potential contaminants prior to testing. The material retained in the SPE trap was subsequently analyzed by gas chromatography–mass spectrometry (GC–MS), and representative oxygenated species are reported in the results section.

A Thermo Scientific HyperSep™ Silica SPE cartridge (1000 mg) was used for this process. The procedure was as follows. An initial 5 mL portion of the fuel sample was passed through the cartridge to precondition the column and then discarded. Subsequently, 25 mL of test fuel was passed through the cartridge under positive pressure to maintain a uniform collection rate. After extraction, the sample was filtered through a fine membrane (0.2 μm) to remove any residual sorbent particles. The cleaned sample was then used directly for ignition delay measurements in the IQT system.

Experimental Setup and Procedure

The ID and DCN measurements were conducted using a CFR Ignition Quality Tester (IQT-LM model) in accordance with ASTM D6890. Traditionally, approximately 150 mL of fuel was required to complete a DCN test, but the new IQT system acquired by Washington State University in 2024 includes manufacturer updates that significantly reduce the fuel volume needed. In this method, the fuel is injected into a heated, temperature-controlled constant-volume combustion chamber (CVCC) pre-charged with compressed air. Each injection triggers a compression ignition event, and the ignition delay defined as the time between the start of fuel injection and the onset of significant combustion is recorded. Each test consists of 15 pre-injections, used to condition the chamber and purge residual fuel, followed by 32 injections from which ignition delay values are averaged. An equation is used to correlate ID to CN using ASTM D613, resulting in a DCN. The Equation B-1 is used when ID ranges from 2.64 ms to 6.90 ms (75.1 DCN to 31.5 DCN).

$$DCN = 4.460 + 186.6/ID \quad \text{(Eq. B-1)}$$

The IQT is able to measure ID outside of this range; however the precision may be affected. When outside the ID range 2.64 ms to 6.90 ms, Equation B-2 should be used for the correlation of ID to DCN.

$$DCN = 83.99(ID - 1.512)^{(-0.658)} + 3.547 \quad \text{(Eq. B-2)}$$

It should be noted that the equation (B-1) and equation (B-2) are not equal at both end points (2.64 ms and 6.90 ms). However, the resolution of this discrepancy is outside the scope of this work. All measurements were calibrated following ASTM protocol using n-heptane (Haltermann solution, 99.86 vol%) with a measured ID of 3.78 ± 0.01 ms and methylcyclohexane (CFR Engine, purity unspecified) with an ID of 10.4 ± 0.5 ms. The charge air pressure was maintained at 310 psi, and the average charge air temperature was 582 ˚C.

Results and Discussion

Experimental Ignition Delay Measurements

Ignition delay measurements were conducted for all six isomers of DMCH and two isomers of decalin using the CFR IQT system, and the corresponding DCNs are summarized in Table B-2. Among the tested DMCH isomers, cis-1,3-DMCH exhibited the highest reactivity, with a DCN of 37.4, while cis-1,2-DMCH showed the lowest reactivity, with a DCN of 21.8. This represents a substantial difference of 15.6 DCN units among structurally similar isomers of DMCH, underscoring the significant influence of both positional and geometric isomerism on ignition behavior.

Table B-2. Ignition delay and DCN of pure compounds.

Compound	Ignition delay, ms	DCN
cis-1,2-DMCH	11.690	21.8
trans-1,2-DMCH	11.404	22.1
cis-1,3-DMCH	5.660	37.4
trans-1,3-DMCH	9.250	25.4
cis-1,4-DMCH	9.742	24.5
trans-1,4-DMCH	7.797	28.6
cis-decalin	5.062	41.3
trans-decalin	6.734	32.2

For the 1,2-substituted isomers, cis-1,2-DMCH and trans-1,2-DMCH yielded nearly identical DCNs of 21.8 and 22.1, respectively. This suggests that geometric isomerism has a negligible effect on ignition delay for 1,2-DMCH. This observation is consistent with values reported in the NREL Compendium of Experimental Cetane Numbers[19], which lists a DCN of 24.0 for a mixed 1,2-DMCH sample. In contrast, the effect of stereochemistry is most pronounced in the 1,3-substituted isomers. The DCN of cis-1,3-DMCH (37.4) is significantly higher than that of trans-1,3-DMCH (25.4), a difference of 12 DCN units. The DCN value of 30.5 reported in the NREL compendium for a mixed 1,3-DMCH sample falls between these two values, further supporting the sensitivity of ignition behavior to stereochemistry in this isomer group. For the 1,4-DMCH isomers, a moderate stereochemical effect is observed. The cis isomer exhibited a DCN of 24.5, whereas the trans isomer reached 28.6, resulting in a difference of 4.1 DCN units. When averaged across stereoisomers, the DCN trend by substitution position follows the order: 1,3-DMCH > 1,4-DMCH > 1,2-DMCH, indicating that positional isomerism also plays a significant role in ignition reactivity, independent of geometry. Figure B-1 summarizes DCN comparison among DMCH isomers.

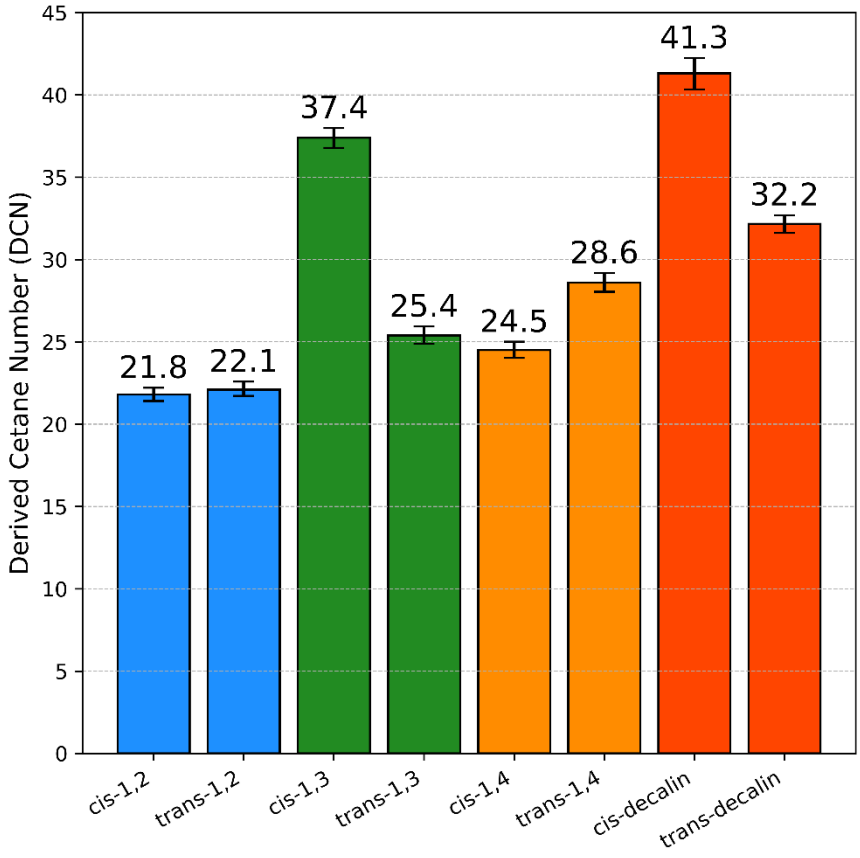

Figure B-1. DCN comparison among DMCH and decalin isomers.

To further validate the role of stereochemistry, cis- and trans-decalin were also evaluated under identical IQT conditions. Cis-decalin yielded a DCN of 41.3, while trans-decalin yielded 32.2—a difference of 9.1 DCN units. These results closely match those of Heyne et al.[10], who reported values of 41.6 and 32.0 for cis- and trans-decalin, respectively.

Possible Kinetic Explanation of DMCH Isomers

The observed variation in DCN among the isomers of DMCH reflects differences in molecular conformation and the corresponding impact on low-temperature oxidation kinetics. These effects are governed by the steric accessibility of hydrogen abstraction sites, the population and stability of reactive conformers, and the propensity for chain-branching pathways such as 1,5-H shifts and β-scission. Collectively, these parameters influence the onset and rate of exothermic radical chemistry that drives low-temperature heat release. The ignition behavior differences among DMCH isomers can be mechanistically explained by examining their molecular conformations, particularly the accessibility of hydrogen abstraction sites and the feasibility of intramolecular hydrogen shifts. Figure B-2 illustrates the most stable chair conformations of the six DMCH isomers, showing the relative positions of methyl groups and highlighting stereochemical effects that influence reactivity.

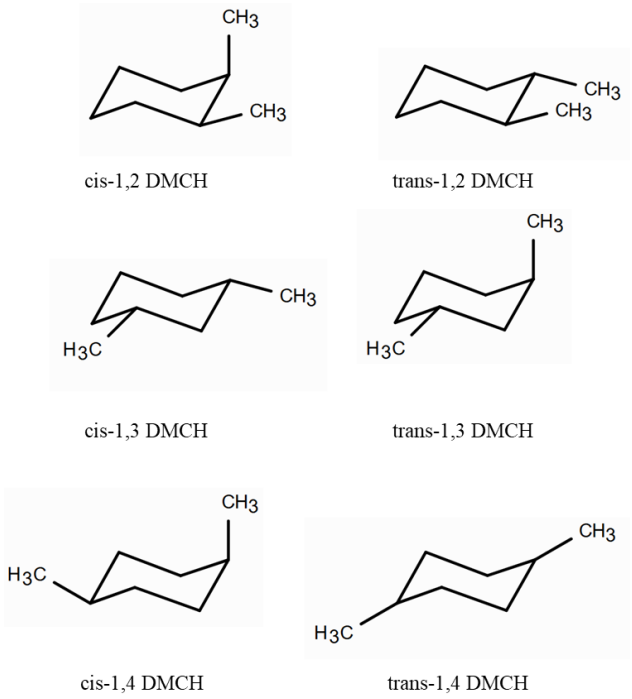

Figure B-2. Chair conformations of six DMCH isomers, highlighting the relative position and stereochemistry of the two methyl groups. Each structure represents the most stable conformer.

Both cis- and trans-1,2-DMCH exhibit similarly low DCNs (~22), indicating that positional substitution at adjacent carbon atoms (C1 and C2) significantly hinders reactivity regardless of stereochemistry. This behavior stems from severe steric congestion between the two methyl groups, which limits access to secondary axial hydrogens, the preferred sites for initial hydrogen abstraction by OH or O_2 radicals[20]. Quantum chemical studies confirm that these isomers predominantly occupy low-energy chair conformers with restricted conformational interconversion. In particular, Bian et al.[21] showed that inversion between conformers in cis-1,2-DMCH involves high energy barriers (>13 kcal/mol), and productive 1,5-H transfer is accessible only in rare, energetically disfavored geometries. Similarly, Sakurai et al.[22] found that radical cation fragmentation in 1,2-DMCH is stereoselective and limited, reinforcing the notion that conformational strain suppresses radical reactivity. Rossini and Pitzer[23] further support this conclusion with thermodynamic data: cis-1,2-DMCH has a higher enthalpy and lower entropy than its trans counterpart, reflecting its greater steric strain and reduced flexibility. Together, these findings indicate that 1,2-substitution locks the molecule into kinetically hindered conformations, reducing the formation of hydroperoxyalkyl radical (QOOH) and other chain-branching intermediates at low temperature.

In contrast, the 1,3-isomers show a pronounced stereochemical influence on DCN. The cis-1,3 isomer exhibits the highest DCN (37.4) of all isomers studied, while the trans form displays significantly lower reactivity (DCN = 25.4). Ab initio studies by Bian et al.[21] demonstrate that cis-1,3-DMCH favors low-energy conformers such as C13Cee, where both methyl groups occupy equatorial positions. This geometry is sterically favorable and facilitates intramolecular 1,5-hydrogen shifts via accessible transition states. At 500 K, the population of this conformer exceeds 99%, ensuring a high likelihood of radical isomerization and early OH regeneration through QOOH pathways. By contrast, trans-1,3-DMCH in its stable chair conformation must adopt an axial–equatorial (C13Cea) geometry due to the trans-1,3 substitution pattern. This configuration leads to more linear molecular geometries that are less favorable for internal hydrogen shift reactions, potentially delaying the onset of OH formation compared to the cis isomer. These conformers restrict chain-branching, delay low-temperature heat release, and result in a lower DCN. This stereochemical dependence on 1,5-H migration is consistent with prior kinetic models by Yang et al.[16], which identify H-shift rates and QOOH formation as sensitive to ring geometry and substituent orientation.

The 1,4-DMCH isomers fall between the extremes observed in 1,2- and 1,3-substitution. Both cis and trans forms exhibit intermediate DCNs, with only a modest difference between stereoisomers. In these structures, the methyl groups are positioned at para-positions, on opposite poles of the cyclohexane ring, which minimizes steric interference and preserves conformational flexibility. Quantum calculations show relatively low energy differences among conformers and lower inversion barriers, suggesting that both isomers maintain access to reactive geometries over a wide temperature range[24]. This pattern is supported by pyrolysis data from Gillespie et al.[25], who found that 1,4-DMCH readily undergoes radical fragmentation via ring hydrogen abstraction, consistent with the structural accessibility of reactive sites in these isomers.

These structure reactivity trends are reinforced by kinetic modeling and flow-reactor studies. Yang et al.[16] showed that 1,2-DMCH is more reactive at high temperatures, where ring-breaking dominates. While 1,3-DMCH exhibits enhanced reactivity under low-temperature conditions due to its propensity for H-migration and QOOH generation. Their sensitivity analyses confirmed that cis-isomers generally promote earlier formation of chain-branching intermediates, correlating with shorter ignition delays and higher DCN.

Temperature and Pressure Dependence of Decalin Isomers

To further investigate the mechanistic differences between cis- and trans-decalin in low temperature oxidation chemistry, a comprehensive series of ID measurements were conducted over a range of temperatures (400-620 ˚C) and pressure (250-350 psi). These conditions span the peroxy radical chemistry and hydrogen shift isomerization regime, allowing detailed investigation of conformational effects. During the temperature sweep, pressure was held constant at 310 psi, while the pressure sweep was performed at a fixed temperature of 450 ˚C, enabling isolated analysis of each variable's influence on ignition behavior.

Figure B-3 illustrates the pressure and temperature dependence of ID for cis- and trans-decalin. The top panel displays strong Arrhenius behavior, with high linearity for both cis- and trans-decalin (R^2 =0.992 and 0.992, respectively). Although both exhibit similar slopes, the cis isomer consistently displays shorter ID times across the entire temperature range studied. This indicates that the overall reactivity of cis-decalin is higher, likely due to greater accessibility of low-temperature chain-branching pathways, particularly below 550 ˚C, where RO_2 and QOOH intermediates play key roles[26-29]. As these reactions involve complex networks rather than single elementary steps, the observed differences in ID may reflect variations in the number or efficiency of reactive pathways available to each isomer, rather than differences in a single activation energy barrier.

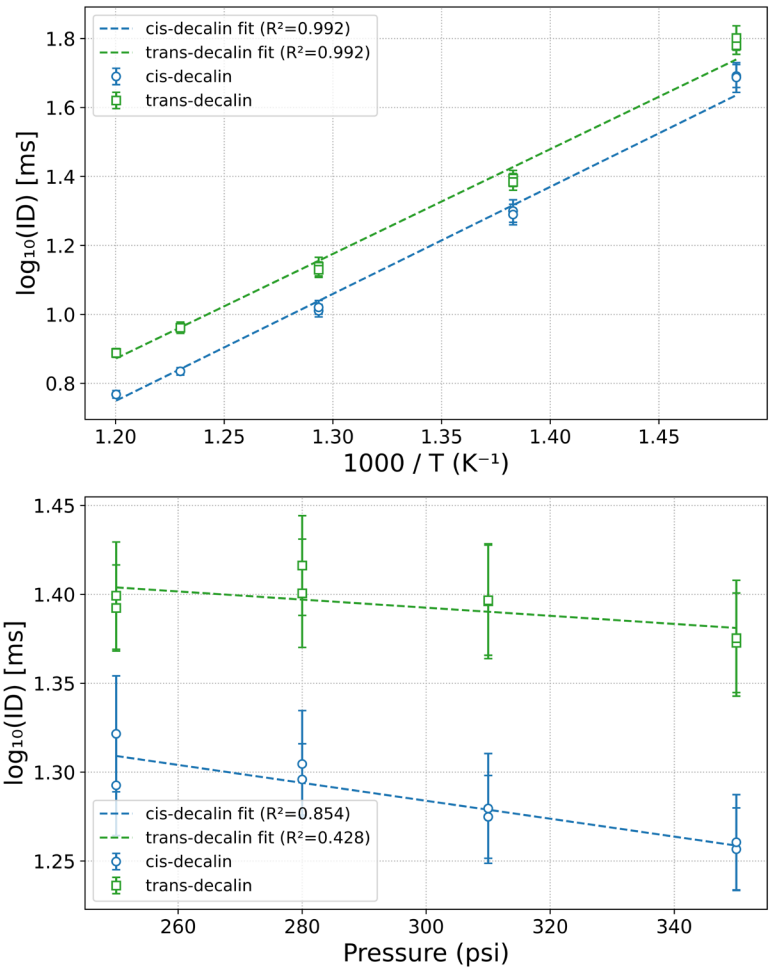

Figure B-3. Pressure and temperature dependence of ignition delay for cis- and trans-decalin. Data points represent duplicate measurements with error bars showing one standard deviation (SD). Each point is the mean of 32 injections; error bars are one SD across injections; two markers at a condition indicate independent duplicate tests. Dashed lines are linear fits to the logarithm of ignition delay, with coefficients of determination (R^2) included in the legend.

The bottom panel of Figure B-3 shows that cis-decalin also exhibits stronger pressure dependence (R^2 = 0.854), while trans-decalin shows weak sensitivity to pressure changes (R^2 = 0.428). This differential response implies that cis-decalin benefits significantly from pressure assisted stabilization of radical intermediates, which is consistent with unimolecular reaction pathways that involve third-body collisions[27,30].

Figure B-4 expands on these observations by directly comparing the ratio of ID (cis/trans-decalin) across temperature and pressure sweeps. In the top panel, the ID ratio decreases slightly with increasing temperature but remains below one across the full range. This reinforces the conclusion that cis-decalin is consistently more reactive, particularly at lower temperatures where peroxy radical isomerization dominates. The weak temperature dependence and low R^2 (0.006) indicate that the ratio of ignition delays between cis- and trans-decalin remains nearly constant across the studied temperature range. This supports the earlier observation that both isomers have similar apparent activation energies in this regime. Each point represents one of many pairwise combinations between individual cis- and trans- measurements, with error bars reflecting the propagated uncertainty from both isomers. The resulting scatter reflects real experimental variability while still preserving the overall trend.

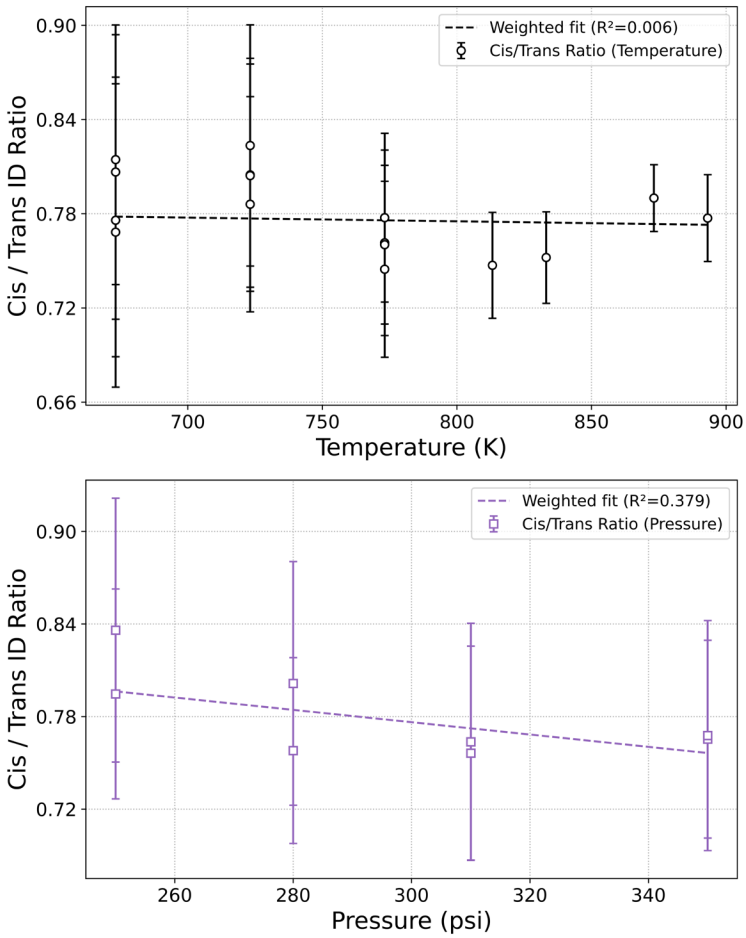

Figure B-4. Effect of temperature and pressure on cis/trans ignition delay ratio of decalin isomers. Data points represent ratios derived from independent replicate measurements of cis- and trans-decalin; error bars were propagated from the replicate standard deviations. Dashed lines show linear fits with R^2 reported in the legend.

In contrast, the bottom panel of Figure B-4 reveals a negative correlation between the ID ratio and pressure ($R^2 = 0.379$). This supports the interpretation that the pressure-enhanced reactivity of cis-decalin is not matched by trans-decalin, likely due to geometric constraints that limit efficient 1,6-H shift isomerization in the trans isomer. As pressure increases, the efficiency of pressure-dependent low-temperature pathways[27,30] (e.g., $RO_2 \rightleftharpoons QOOH$ and O_2QOOH formation) disproportionately benefits cis-decalin, driving the ratio lower. Figure B-5 illustrates a representative 1,5-H abstraction transition state in cis-decalin, where axial hydrogen accessibility supports faster QOOH formation under low-temperature and high-pressure conditions.

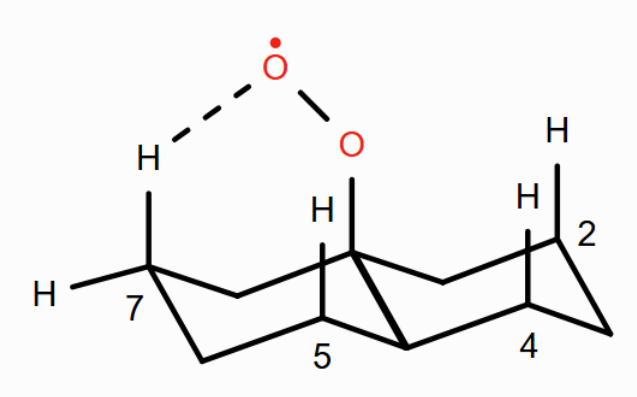

Figure B-5. Illustration of a 1,5-hydrogen abstraction transition state in cis-decalin. The axial hydrogen at the 7-position is abstracted by a peroxy radical (ROO·), initiating QOOH formation. The adjacent equatorial hydrogen and other abstractable sites are shown for reference. This geometry supports efficient low-temperature chain branching, consistent with the enhanced reactivity and pressure sensitivity observed experimentally. Adapted from Heyne et al.[10]

Taken together, the temperature and pressure dependence of ID in cis- vs. trans-decalin highlight the mechanistic role of H-shift pathways. The data support a scenario where 1,5-H shift isomerization in cis-decalin is more accessible and pressure-enhanced, whereas trans-decalin is constrained to slower or less pressure-responsive 1,6-H pathways. These insights clarify the structure-reactivity relationship and aid in modeling low-temperature oxidation behavior of bicyclic hydrocarbons. A full computational treatment of the isomer-dependent oxidation pathways lies beyond the scope of this work, but represents an important avenue for future study.

Polar Contaminant Effect on Ignition Delay

Trace polar species, particularly peroxides and oxygenates, are well known to accelerate low temperature combustion chemistry and reduce ID. These compounds can form during ambient storage through slow autoxidation of hydrocarbons in the presence of oxygen, and even at ppm levels, they can significantly bias DCN measurements by promoting radical generation and chain branching.

To assess this effect, each DMCH isomer was tested immediately upon opening (“as received”), then stored under ambient, light-protected conditions for 135 days in sealed amber bottles (although no purge using inert gas was performed). No further purification was applied prior to re-testing. Figure B-6 compares ID values before and after storage, with error bars representing standard deviations from 32 injections per test.

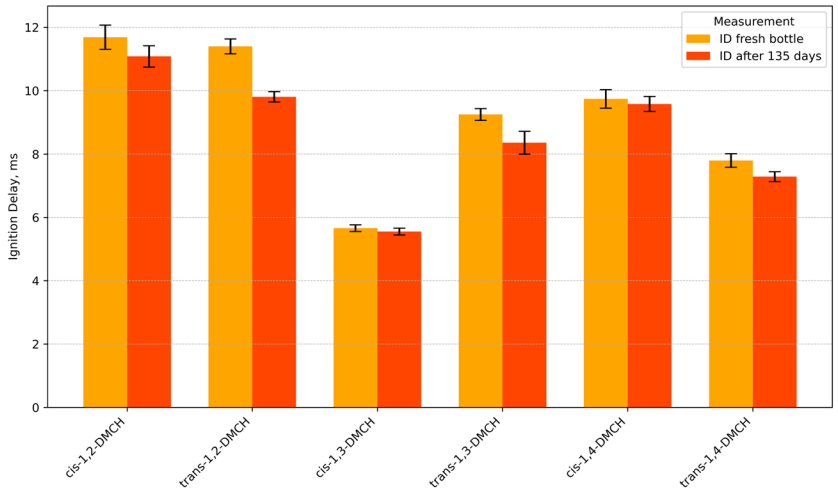

Figure B-6. Ignition delay comparison of DMCH isomers before and after 135 days of storage.

Among the DMCH isomers, trans-1,2-DMCH showed the most significant ID reduction from 11.40 ms to 9.81 ms, well beyond experimental uncertainty. Smaller but measurable decreases were also observed for trans-1,3-DMCH and trans-1,4-DMCH. In contrast, the cis isomers exhibited less change over time, indicating greater oxidative (storage) stability which is likely due to conformational constraints that hinder peroxide formation or radical propagation.

A similar trend was observed in trans-decalin, which initially showed an abnormally low ID of 5.33 ms (DCN = 39.5), inconsistent with literature values (≈32). Following SPE to remove polar contaminants, the ID increased to 6.73 ms (DCN = 32.2), aligning with prior reports and confirming that oxidative degradation had artificially enhanced the sample's reactivity. This validates both the susceptibility of trans-fused cycloalkanes to oxidative change and the efficacy of SPE purification.

GC-MS analysis of the SPE retained polar fraction from trans-decalin confirmed the presence of multiple oxygenated species, including ketones and hydroxylated decalin derivatives, further supporting the hypothesis that oxidative byproducts were responsible for the observed ID reductions. A full chromatogram, annotated peak identities, and mass spectra are provided in Supplemental Information (SI). It should be noted that while SPE GC-MS analysis is qualitative in nature, these results reinforce the need for careful fuel handling and purification when evaluating ignition properties particularly for fuels prone to peroxide formation. This is especially important for accurate kinetic model validation and experimental repeatability in surrogate fuel testing. The scope of this polar study is not to quantify the kinetics or concentrations of these impurities, but rather to alert the community to their potential impact on ignition measurements.

It should be noted that while the IQT provides a standardized and certification relevant platform for ignition delay and DCN determination, it does not capture the full range of autoignition behavior accessible with complementary equipment such as shock tubes or rapid compression machines. IQT measurements are most sensitive to mid temperature reactivity, whereas low-temperature chain branching and high-pressure kinetics are better resolved by other devices. Thus, while the present work emphasizes relative trends among isomers under ASTM D6890 conditions, a broader mechanistic picture will require integration with complementary methods in future studies. Although a comprehensive ab initio calculation/kinetic modeling of the isomer dependent oxidation network (conformers, H-abstraction sites, RO_2/QOOH isomerization, and pressure effects) would be valuable, it lies beyond the scope of this experimental study and would constitute a separate contribution. Here we focus on delivering an isomer-resolved, internally consistent IQT dataset under certification-relevant conditions (ASTM D6890), together with a literature based mechanistic context that can be used to benchmark and refine future models and surrogate fuel formulations.

Conclusion

Here, we investigated the impact of stereochemistry on the ID behavior of DMCH isomers. Among the isomers tested, cis-1,3-DMCH exhibited the highest reactivity, with a DCN of 37.4, while cis-1,2-DMCH was the least reactive, with a DCN of

21.8. The most pronounced stereochemical effect was observed between cis- and trans-1,3-DMCH, which showed a significant DCN difference of 12.0. In contrast, the effect was minimal for cis- and trans-1,2-DMCH, with only a 0.3 DCN difference. These variations are attributed to differences in molecular conformation, which directly influence low-temperature oxidation pathways and the formation of reactive intermediates during combustion.

To validate and extend these findings, cis- and trans-decalin were examined under a range of temperatures and pressures. Cis-decalin consistently exhibited faster ignition and stronger pressure sensitivity, consistent with its ability to access more favorable low-temperature chain-branching mechanisms (e.g., 1,5-H shift). The trans isomer, in contrast, was limited by conformational rigidity and exhibited weaker pressure dependence, likely due to inefficient 1,6-H isomerization. These results clarify the mechanistic basis for structure-reactivity trends among fused bicyclic hydrocarbons.

We also evaluated the impact of trace polar contaminants formed during ambient storage. Trans isomers, particularly trans-decalin, showed notable ignition delay reductions due to oxidative degradation. SPE and GC-MS confirmed the presence of oxygenated byproducts, such as ketones and hydroxylated species. These findings underscore the need for careful sample preparation to ensure accurate ignition property comparisons across isomer classes.

Taken together, these findings demonstrate that molecular stereochemistry and positional isomerism play critical roles in governing ignition behavior. This work deepens the mechanistic understanding of structure-reactivity relationships in cycloalkanes and offers valuable guidance for surrogate fuel formulation, SAF pathway evaluation, and chemical kinetic model development. Although this study focused on pure cis- and trans-cycloalkanes, such measurements are directly relevant to multi component SAF mixtures. Because DCN typically follows a linear by volume blending rule, accurate pure-component data expand the DCN database and support both hydrocarbon type analysis and quantitative structure property relationship (QSPR) modeling. These insights help address knowledge gaps on cycloalkanes and strengthen confidence in their role within sustainable aviation fuel blending strategies.

References

[1] US DOE. USDA, EPA, US Department of Transportation. (2022). *SAF Grand Challenge Roadmap*. https://www.energy.gov/eere/bioenergy/articles/sustainable-aviation-fuel-grand-challenge-roadmap-flight-plan-sustainable

[2] European Union. (2023). *Regulation - EU - 2023/2405 - EN - EUR-Lex*. https://eur-lex.europa.eu/eli/reg/2023/2405/oj

[3] Colket, M., & Heyne, J. (2021). *Fuel Effects on Operability of Aircraft Gas Turbine Combustors*. American Institute of Aeronautics and Astronautics, Inc., https://doi.org/10.2514/4.106040

[4] Luecke, J., Naser, N., Yang, Z., Heyne, J., & McCormick, R. L. (2025). Measurement of Spray Chamber Ignition Delay and Cetane Numbers for Aviation Turbine Fuels. *Energy and Fuels, 39*(22), 10479-10487. https://doi.org/10.1021/acs.energyfuels.5c01350

[5] ASTM International. (2022). *ASTMD4054: Standard Practice for Evaluation of New Aviation Turbine Fuels and Fuel Additives*. https://doi.org/10.1520/D4054-22

[6] Boehm, R. C., Colborn, J. G., & Heyne, J. S. (2021). Comparing Alternative Jet Fuel Dependencies Between Combustors of Different Size and Mixing Approaches. *Front. Energy Res. 9*, 440. https://doi.org/10.3389/FENRG.2021.701901

[7] Ruan, H., Qin, Y., Heyne, J., Gieleciak, R., Feng, M., & Yang, B. (2019). Chemical Compositions and Properties of Lignin-Based Jet Fuel Range Hydrocarbons. *Fuel, 256*, 115947. https://doi.org/10.1016/j.fuel.2019.115947

[8] Yang, Z., Xu, Z., Feng, M., Cort, J. R., Gieleciak, R., Heyne, J., & Yang, B. (2022). Lignin-Based Jet Fuel and Its Blending Effect with Conventional Jet Fuel. *Fuel, 321*, 124040. https://doi.org/10.1016/j.fuel.2022.124040

[9] Kubic, W. L. (2016). *A Group Contribution Method for Estimating Cetane and Octane Numbers*. https://doi.org/10.2172/1291241

[10] Heyne, J. S., Boehman, A. L., & Kirby, S. (2009). Autoignition Studies of Trans- and Cis-Decalin in an Ignition Quality Tester (IQT) and the Development of a High Thermal Stability Unifuel/Single Battlefield Fuel. *Energy and Fuels, 23*(12), 5879–5885. https://doi.org/10.1021/ef900715m

[11] Kang, D., Kirby, S., Agudelo, J., Lapuerta, M., Al-Qurashi, K., & Boehman, A. L. (2014). Combined Impact of Branching and Unsaturation on the Autoignition of Binary Blends in a Motored Engine. *Energy and Fuels, 28*(11), 7203–7215. https://doi.org/10.1021/ef501629p

[12] Kang, D., Lilik, G., Dillstrom, V., Agudelo, J., Lapuerta, M., Al-Qurashi, K., & Boehman, A. L. (2015). Impact of Branched Structures on Cycloalkane Ignition in a Motored Engine: Detailed Product and Conformational Analyses. *Combust. Flame, 162*(4), 877–892. https://doi.org/10.1016/j.combustflame.2014.09.009

[13] Yang, M., & Wang, J. (2024). Comprehensive Multipath Variational Kinetics Study on Hydrogen Abstraction Reactions from Three Typical Dimethylcyclohexane Isomers by Hydroxyl Radicals: From the Electronic Structure to Model Applications. *J. Phys. Chem. A, 128*(22), 4517–4531. https://doi.org/10.1021/acs.jpca.4c00480

[14] Abdul Jameel, A. G., Naser, N., Emwas, A. H., Dooley, S., & Sarathy, S. M. (2016). Predicting Fuel Ignition Quality Using 1H NMR Spectroscopy and Multiple Linear Regression. *Energy and Fuels, 30*(11), 9819–9835. https://doi.org/10.1021/acs.energyfuels.6b01690

[15] Do, P. T., Alvarez, W. E., & Resasco, D. E. (2006). Ring Opening of 1,2- and 1,3-Dimethylcyclohexane on Iridium Catalysts. *J. Catal., 238*(2), 477–488. https://doi.org/10.1016/j.jcat.2005.12.021

[16] Yang, M., Liang, Y., & Wang, J. (2025). A Comparative Experimental and Kinetic Modeling Study on the Oxidation Chemistry of 1,2- and 1,3-Dimethylcyclohexanes: Key Cyclic Components in Sustainable Biofuels and Fossil Fuels. *Fuel, 387*, 134417. https://doi.org/10.1016/j.fuel.2025.134417

[17] Rosado-Reyes, C. M., & Tsang, W. (2014). Isomerization of Cis-1,2-Dimethylcyclohexane in Single-Pulse Shock Tube Experiments. *J. Phys. Chem. A, 118*(36), 7707–7714. https://doi.org/10.1021/jp505305y

[18] Boehm, R. C., Yang, Z., & Heyne, J. S. (2022). Threshold Sooting Index of Sustainable Aviation Fuel Candidates from Composition Input Alone: Progress toward Uncertainty Quantification. *Energy & Fuels, 36*(4), 1916-1928. https://doi.org/10.1021/acs.energyfuels.1c03794

[19] Yanowitz, J., Ratcliff, M. A., Mccormick, R. L., Taylor, J. D., & Murphy, M. J. (2017). *Compendium of Experimental Cetane Numbers*. Golden.

[20] Klimkowski, V. J., Manning, J. P., & Schafer, L. (1985). Molecular Structures and Intramolecular Interactions in Dimethyl Cyclohexane Isomers. *J. Comput. Chem., 6*(6), 570–580.

[21] Bian, H., Ye, L., Li, J., Sun, J., Liang, T., Zhong, W., & Zhao, J. (2019). Impact of Conformational Structures on Primary Decomposition of Cis-1,2-Dimethylcyclohexyl Isomers: A Theoretical Study. Combust. *Flame, 205*, 193–205. https://doi.org/10.1016/j.combustflame.2019.04.024

[22] Sakurai, H., Shiotani, M., & Ichikawa, T. (1999). Hydrogen Molecule Detachment in Irradiated 1,2-Dimethyl Cyclohexane: Stereo-Selective Reaction. *Radiat. Phys. Chem., 54*(3), 235–240. https://doi.org/10.1016/S0969-806X(98)00257-6

[23] Rossini, F. D., & Pitzer, K. S. (1947). Relabeling of the Cis and Trans Isomers of 1,3-Dimethylcyclohexane. *Science, 105*(2738), 647. https://doi.org/10.1126/science.105.2738.647

[24] Bian, H., Zhang, Y., Wang, Y., Zhao, J., Ruan, X., & Li, J. (2021). Computational Study of Inversion-Topomerization Pathways in 1,3-Dimethylcyclohexane and 1,4-Dimethylcyclohexane: Ab Initio Conformational Analysis. *Int. J. Quantum Chem., 121*(11), 1–13. https://doi.org/10.1002/qua.26636

[25] Gillespie, H. M., Gowenlock, B. G., & Johnson, A. F. (1979). The Pyrolysis of Cyclic Hydrocarbons. Part 1. 1.4-Dimethylcyclohexane. *J. Chem. Soc. Perkin Trans., 2*, 317-324.

[26] Burke, U., Somers, K. P., O'Toole, P., Zinner, C. M., Marquet, N., Bourque, G., Petersen, E. L., Metcalfe, W. K., Serinyel, Z., & Curran, H. J. (2015). An Ignition Delay and Kinetic Modeling Study of Methane, Dimethyl Ether, and Their Mixtures at High Pressures. *Combust. Flame, 162*(2), 315–330. https://doi.org/10.1016/j.combustflame.2014.08.014

[27] Zádor, J., Taatjes, C. A., & Fernandes, R. X. (2011). Kinetics of Elementary Reactions in Low-Temperature Autoignition Chemistry. *Prog. Energy Combust. Sci., 37*(4), 371–421. https://doi.org/10.1016/j.pecs.2010.06.006

[28] Peeters, J., Nguyen, T. L., & Vereecken, L. (2009). HOx Radical Regeneration in the Oxidation of Isoprene. *Phys. Chem. Chem. Phys., 11*(28), 5935–5939. https://doi.org/10.1039/b908511d

[29] Westbrook, C. K., Pitz, W. J., Herbinet, O., Curran, H. J., & Silke, E. J. (2009). A Comprehensive Detailed Chemical Kinetic Reaction Mechanism for Combustion of N-Alkane Hydrocarbons from n-Octane to n-Hexadecane. *Combust. Flame, 156*(1), 181–199. https://doi.org/10.1016/j.combustflame.2008.07.014

[30] Glowacki, D. R., Wang, L., & Pilling, M. J. Evidence of Formation of Bicyclic Species in the Early Stages of Atmospheric Benzene Oxidation. *J. Phys. Chem. A, 113*(18), 5385–5396. https://doi.org/10.1021/jp9001466